

Advanced linear modeling and interpolation in CT-reconstruction

Per-Erik Danielsson and Johan Sunnegårdh

Abstract—Although not so often expressed as a modeling problem neither projection nor back-projection can be designed without certain insights in the physics of CT. However, most of this insight is left aside, since it is generally believed that only the most simplified models can be included in the innermost time-consuming loop in projection and back-projection.

We propose that any linear projection procedure should model three functions: The irradiation function, the footprint/basis function, and the gantry rotation function. We demonstrate how a moderately advanced modeling of these three functions can be brought together in an interpolation procedure and yield a surprisingly efficient inner loop interpolation. To this end we *i)* carefully select a locus of interpolation path through image and projection data spaces and *ii)* execute multiple convolution as integration by parts implemented by table-look-up.

Index Terms—Linear models, CT-projection, Irradiation function, Table-look-up.

I. INTRODUCTION

The most time-critical loops in CT-reconstruction are interpolations embedded in projection and/or back-projection. The simplest techniques go by the name of nearest neighbor and linear interpolation. In a projection/backprojection operator the interpolation between the sampled input/output signal (the digital image) and the sampled output/input signal (the detector array) can always be described as convolution of the input with a continuous interpolation function followed by sampling of the result. In a CT-system with a rotating gantry, *this interpolation function is always a convolution of the following three functions*, although in simple interpolation techniques, some or all of the three are made invisible by assuming them to be Dirac functions.

- $i_{l,\gamma}(t)$, the irradiation function describing the cross-section photon flux density in the channel between the beam-spot and a detector element, a function that is bound to vary with the distance l to the source.
- $w_\theta(t)$ is the footprint (the x-ray transform) of the pixel basis function, which may vary with the angle θ in a Cartesian grid.

- $g_\gamma(t)$, the gantry rotation function, which in the form of Δ_θ expresses a time integration interval. $g_\gamma(t)$ varies greatly with the fan angle γ .

The common argument for all three functions is t along which convolution integral is to be evaluated. In many cases this is the detector axis. We assume that the functions may appear in several versions depending on at least one parameter. Thus, $w_\theta(t)$ might vary with the inclination angle θ between the projection ray and the Cartesian grid, as is the case with Joseph interpolation, $i_{l,\gamma}(t)$ varies with the distance l to the source, and the variation in $g_\gamma(t)$ can be attributed to a moving pixel relative to a fixed measurement system during time integration, or the other way around, a movement of the irradiation system relative to the fixed object pixel.

The simplest model for any of these three functions is a Dirac. For instance, a common back-projection interpolation function assumes that both $w_\theta(t)$ and $g_\gamma(t)$ are Dirac functions while the adopted irradiation function is $i(t) = \Delta_t^{-1} \mathcal{A}(t \Delta_t^{-1})$, a triangle function with unit area. This is a “strip” integral albeit with triangular cross-section having no variation on its path from source to detector. In the light of the above, there is a host of other possibilities, which could emulate the physical process in much more detail. The following two things might hold us back in these attempts.

1) A linear model, however sophisticated, cannot take into account a non-linear data capture process, which includes the exponent-sum-logarithm. To include this non-linearity it is common to employ sub-resolution modeling in the form of multiple ray-tracing. Sub-resolution with a factor of 3 in all dimensions multiplies the number of rays with the factors 27 and 243 in the fan-beam and cone-beam cases, respectively. Hence, such non-linear modeling is expensive indeed.

2) For linear and non-linear models alike, the more sophisticated, the more costly it gets.

We intend to arrange the loop-structure of the interpolation so that we follow a vertical line in the xy-plane, in Fig 2a) called the *locus of inner loop interpolation*. As a result, from now on all three functions have the y -coordinate rather than t or the detector array angle γ as their main attribute.

This work was supported by Siemens Medical Solutions, Forchheim, Germany. The authors are with the Computer Vision Laboratory, Dept. of Electrical Engineering, Linköping Universitet, SE-581 83 Linköping, Sweden. E.mail: ped@isy.liu.se

II. THE THREE FUNCTIONS

A. The irradiation function $i(\gamma, y)$

Fig.1 illustrate the attempt to model the photon density in the channel between beam-spot and a detector element with the 2D-function $i_l(t)$. The cross-section changes relatively slowly along the ray and we can safely assume that it is constant over the actual pixel neighborhood. Therefore, we have downgraded the coordinate l to appear as an index parameter. The irradiation function emanates as the convolution of two aperture functions f_{BA} and f_{DA} describing the photon emission variation over the beam-spot and the detector sensitivity over the detector element, respectively. If these aperture functions are rectangles, the $i_l(t)$ cross-sections appear as illustrated by Fig.1.

Designers of CT-systems try to place the most narrow, and nearly triangular cross-section precisely in the iso-center to maximize the system bandwidth. Let us first simplify this model by making the two apertures identical and equal to Δ_t . Furthermore, we assume that the cross-section is shaped as the triangle function $2\Delta_t^{-1}\mathcal{A}(2t\Delta_t^{-1})$ for the most part of the path between beam spot and detector. Projected onto the locus line, the triangle becomes stretched out with the factor $\cos(\theta+\gamma)$ yielding the function $2\Delta_t^{-1}\cos(\theta+\gamma)\mathcal{A}(2y\cos(\theta+\gamma)\Delta_t^{-1})$.

Our goal is to model fan-beam projection. Detailed modeling of projection/back-projection in parallel beam geometry is of limited interest, since the preceding rebinning operation acts like a smoothing screen between the reconstruction operation and the real fan-beam data. The global fan-beam geometry creates overlap between neighboring irradiation functions, as shown in Fig. 3, which calls for the weighting factor lR^{-1} , the distance relation between the source-to-pixel distance l and the source-to-detector distance R . The final function then yields

$$i(\gamma, y) = lR^{-1}2\cos(\theta+\gamma)\Delta_t^{-1}\mathcal{A}(2y\cos(\theta+\gamma)\Delta_t^{-1}) \quad (1)$$

From the geometry in Fig. 2a) also follows that

$$i(\gamma, y) = 2(R_{iso}\cos\theta+x_p)\Delta_t^{-1}\mathcal{A}(y2\cos(\theta+\gamma)\Delta_t^{-1}) \quad (2)$$

B. The Joseph footprint function [1], $w(\gamma, y)$

Over the interval $-\frac{\pi}{4} < \theta + \gamma \leq \frac{\pi}{4}$, this footprint function is a triangle of constant area $1 \cdot \Delta_y$, the base and height of which varies in the ray direction as $\Delta_y \cos(\theta + \gamma)$ and, $\cos^{-1}(\theta + \gamma)$, respectively. When mapped onto the locus of interpolation line the base becomes constant and equal to Δ_y , which yields the convolution kernel

$$w(\gamma, y) = \mathcal{A}(y\Delta_y^{-1}) \quad (3)$$

C. The gantry rotation function $g(x_p, y)$

In Fig.2a) we find the gantry rotation indicated as a time integrating rectangle function $r\Delta\theta$ along the periphery of the circle with radius r over the measurement interval $\Delta\theta$. The base of the rectangle function projected onto the locus-of-interpolation line is reduced to $r\Delta\theta \cos\phi = \Delta\theta x_p$, proportional to the velocity component, a velocity component which is common for all points along the locus line. In the enlarged detail inset Fig.2b) this projection is done, yielding the rectangle function (4) with smaller width but the same area as the original time integral $\Delta\theta$, ready to slide (be convolved) down the locus line.

$$g(x_p, y) = x_p^{-1}\mathcal{R}(y(\Delta\theta x_p)^{-1}) \quad (4)$$

III. INTERPOLATION AND CONVOLUTION WITH TABLE LOOK-UP

We denote the complete interpolation function as $h(y)$ being the convolution of the above three functions projected onto the locus line with the independent coordinate y . Using (1) the total interpolation function yields

$$h(\gamma, y) = i(\gamma, y) * w_\gamma(y) * g_{x_p}(y) = 2lR^{-1}2\cos(\theta+\gamma)\Delta_t^{-1}x_p^{-1} \mathcal{A}(2y\cos(\theta+\gamma)\Delta_t^{-1}) * \mathcal{A}(y\Delta_y^{-1}) * \mathcal{R}(y(\Delta\theta x_p)^{-1}) \quad (5)$$

Alternatively, using (2) instead of (1) we obtain

$$h(\gamma, y) = 2(R_{iso}\cos\theta+x_p)\Delta_t^{-1}x_p^{-1} \cdot \mathcal{A}(2y\cos(\theta+\gamma)\Delta_t^{-1}) * \mathcal{A}(y\Delta_y^{-1}) * \mathcal{R}(y(\Delta\theta x_p)^{-1}) \quad (6)$$

Since all parameters in the top line of (6) are constant on the locus-of-interest line there should be no problem to evaluate this quantity in the innermost loop. The first kernel in the second line is the triangle function $2\cos^{-1}(\theta+\gamma)\Delta_t^{-1}$, a quantity which we evaluate in one table look-up. For the actual evaluation of the convolution we proceed as follows.

The bottom row is separated into two parts, namely

$$\begin{aligned} h_d &= \mathcal{A}(2y\cos(\theta+\gamma)\Delta_t^{-1}) \\ h_p &= \mathcal{A}(y\Delta_y^{-1}) * \mathcal{R}(y(\Delta\theta x_p)^{-1}) \end{aligned} \quad (7)$$

Consider h_d as located on the locus line in (x_p, y_d) , where the ray γ_d is hitting the center of the detector element γ , while h_p is located where the ray γ_p hits the center of a pixel at the grid-point (x_p, y) as illustrated in Fig. 2b). Clearly, knowing the intercept $y_d - y_p$ enables us to find the coefficient

$$c_{x_p, y_p, \theta, \gamma} = (h_d * h_p)(y_d - y_p) \quad (8)$$

by which the pixel (detector element) value shall be multiplied to yield a contribution to the detector element (θ, γ_d) .

V. DISCUSSIONS AND CONCLUSIONS

For the most part, we have been using a running example to illustrate what we believe is a novel approach to incorporate moderately advanced modeling in a CT-projection operator. Here, we make room for some generalizations. An obvious extension is to accept that the irradiation function h_d has a trapezoidally varying cross-section as illustrated in Fig. 1. The final convolution/interpolation coefficient in will then contain four instead of three terms and the pre-computed table (10) will deliver a quadruple output of y -values.

Everything brought forward here for the fan-beam case can be transported directly to the cone-beam case, provided the irradiation and the footprint functions are separable in horizontal and vertical direction. In the vertical direction there is no rotation but the divergence has to be treated in the same way as above. We should put together an interpolation function that is the convolved result of a foot-print function, e.g. a triangle function $\cos^{-1}(\kappa)\mathcal{A}(z\mathcal{A}_z^{-1})$, where κ is the cone-beam angle, and an irradiation function that describes the variation of photon flux density in the vertical direction of the channel between beam-spot and the detector. The quality improvement brought about with this technique is described by Sunnegårdh [9].

All interpolation functions designed after this recipe will automatically retain a projection-backprojection symmetry, a feature with several benefits in iterative reconstruction as recently brought forward by Ziegler et al [8]. Among these are better insight of convergence phenomena [5] and automatic suppression of DC-aliasing [4]. There are no principle problems to replace the function $w(\gamma, y)$ in (3) with more sophisticated footprint functions [6], [7], which suppress aliasing even better, at the expense of larger processing time due to their wider kernels.

REFERENCES

- [1] P. M. Joseph, An improved algorithm for reprojection rays through pixel images. *IEEE Transactions of Medical Imaging*, 1:193-196, June 1982
- [2] K. M. Hanson and G. W. Wecksung. Local basis-function approach to computed tomography, *Applied Optics*, 24(23): 4028-4039, Dec. 1985
- [3] P.E. Danielsson and M. Magnusson Seger. A proposal for combining FBP and ART in CT-reconstruction. 7th Int. Meeting on fully 3D image reconstruction, St Malo, France, July 2003
- [4] B. De Man and S. Basu, Distance-driven projection and back-projection in three dimensions, *Physics in Medicine and Biology*, 49:2463-2475
- [5] G. L. Zeng and G. T. Gullberg. Unmatched projector/backprojector pairs in an iterative reconstruction algorithm. *IEEE Transaction of Medical Imaging*, 19(5), 548-555 2004
- [6] R. M. Lewitt, Multi-dimensional digital image representations using generalized Kaiser-Bessel window functions, *Journal of the Optical Society of America*, 7(10) Oct. 1982
- [7] M. Magnusson Seger. Three-dimensional reconstruction from cone-beam data using an efficient Fourier technique combined with a special interpolation filter. *Phys. Med. Biol.* **43** (1998) 951-959
- [8] A. Ziegler, Thomas Köhler, Tim Nielsen, and Roland Proksa, Iterative cone-beam CT image reconstruction with spherical symmetrical basis functions, 8th Int. Meeting on fully 3D image reconstruction, Salt Lake City, US, July 2005
- [9] J. Sunnegårdh, A new anti-aliased projection operator for iterative CT reconstruction. In (*ibid*)

To avoid all convolution operations we are now going to employ the technique first suggested for interpolation purposes by Hanson and Wecksung [2], and which can be shown to be equivalent to integration-by-parts. The main idea is shown by Fig.4. A function, which can be separated into one (arbitrary complex) finite function such as h_p in (6) convolved with a rectangle function, $D^{-1}\mathcal{R}(yD^{-1})$ can be evaluated at the arbitrary point $y = y_1$ using table look-up in the function $H_1(y) \equiv \int_{-\infty}^y h(y')dy'$ as $H_1(y_1 + \frac{D}{2}) + H_1(y_1 - \frac{D}{2})$. By the same token, since a triangle function $D^{-1}\mathcal{A}(yD^{-1})$ is the convolution of two identical rectangle functions, we can take the idea one step further by computing and tabulating $H_2(y) \equiv \int_{-\infty}^y H_1(y')dy'$. The corresponding convolution result then yields

$$H_2(y_1 - D) - 2H_2(y_1) + H_2(y_1 + D) \quad (9)$$

IV. THE INNER LOOP INTERPOLATION FOR PROJECTION

Since the detector element aperture is $\mathcal{A}_t = R\mathcal{A}_\gamma$, for each angular step \mathcal{A}_γ the central ray in the irradiation function takes a vertical step in the y -direction along the locus line, which amounts to

$$\mathcal{A}_{y_p} = \mathcal{A}_\gamma (R_{iso} \cos \theta + x_p) \cos^{-2}(\theta + \gamma) \quad (10)$$

which can be verified geometrically in Fig.2. We use (10), or rather the integral thereof to get impact points $y_{\gamma_0}, y_{\gamma_1}, y_{\gamma_2}, \dots$ in continuous coordinates. for all central rays $\gamma_0, \gamma_1 = \gamma_0 + \mathcal{A}_\gamma, \gamma_2 = \gamma_0 + 2\mathcal{A}_\gamma \dots$ of the discrete fan-beam. In addition we tabulate the two impact points of the end points of the triangular kernel that goes with each beam so that the table delivers a triple output of y -coordinates for each γ -entry. At the real detector, these three corresponding points are centers of non-overlapping apertures. On the locus line, however, they do overlap because of the fan-beam and the acute angle ray impact. Now, every grid-point (x_p, y_p) has a contribution $f(x_p, y_p)$ to deliver and an interval \mathcal{A}_{y_p} , which corresponds to the interval D in (9) and brings about the computation

$$p(\theta, \gamma) = p(\theta, \gamma) + f(x_p, y_p) \left[\begin{array}{l} + H_2\left(y_p - y_{\gamma_0} - \frac{\mathcal{A}_y}{\cos(\theta - \gamma)}\right) \\ - 2H_2\left(y_p - y_{\gamma_0}\right) \\ + H_2\left(y_p - y_{\gamma_0} + \frac{\mathcal{A}_y}{\cos(\theta - \gamma)}\right) \end{array} \right]$$

which takes four table-look-ups (one to get the three address increments in parallel) and three to get the total coefficient for the accumulation.

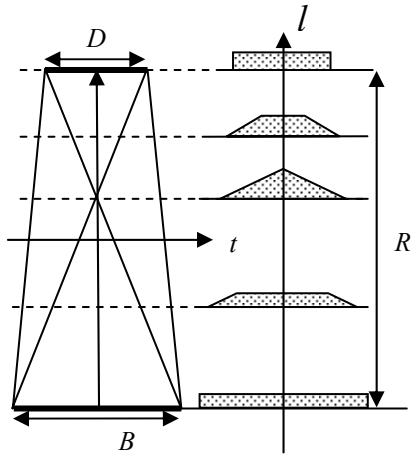


Fig. 1 2D-irradiation function

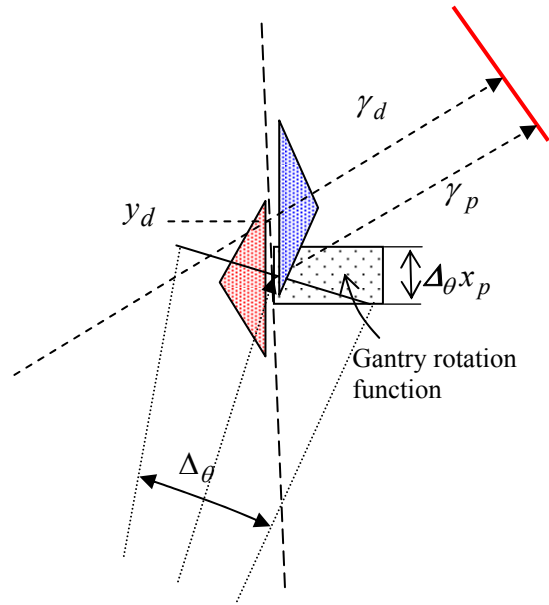


Fig. 2b) Enlargement of detail in 2a)

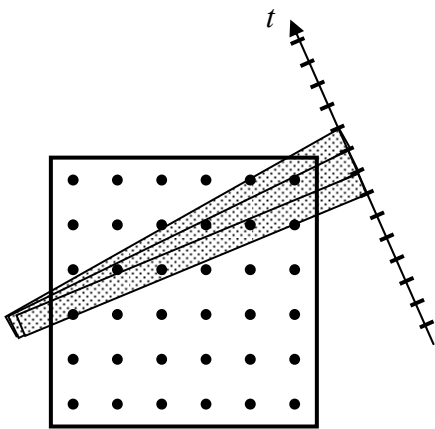


Fig. 3. Overlapping irradiation in fan-beam projection

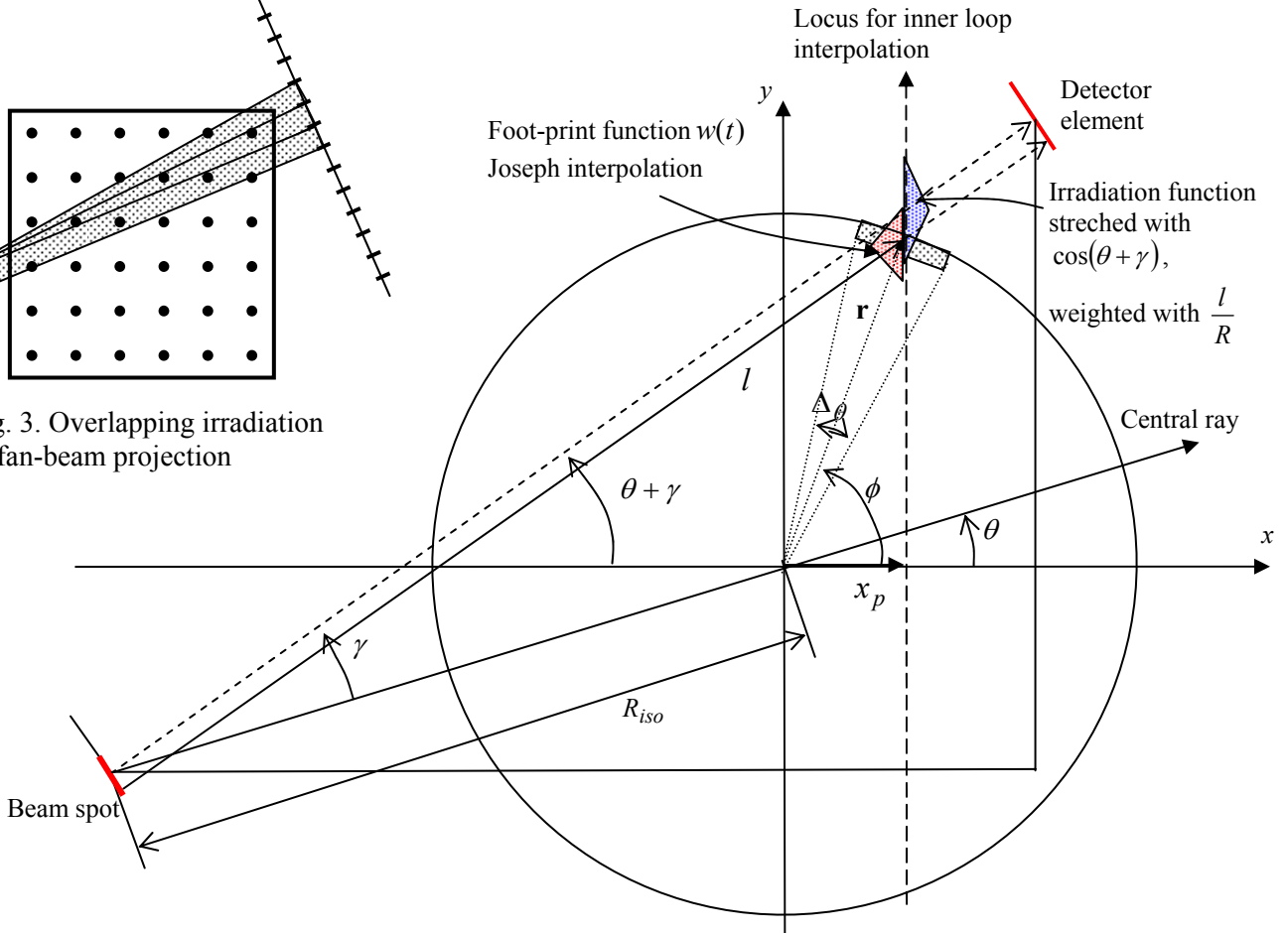


Fig. 2 a). Interpolation functions projected onto locus-of-interpolation line

Fig. 4. Interpolation-convolution between a rectangle function and tabulated function integral

